Negative-ion/positive-ion coincidence spectroscopy as a tool to identify anionic fragments: The case of core-excited CHF_3

A. Kivimäki[1,2], C. Stråhlman[3,2], R. Sankari[4,2], R. Richter[5]

[1]*Nano and Molecular Systems Research Unit, University of Oulu, 90014 Oulu, Finland*
[2]*MAX IV Laboratory, Lund University, 22100 Lund, Sweden*
[3]*Department of Materials Science and Applied Mathematics, Malmö University, 20506 Malmö, Sweden*
[4]*Surface Science Group, Laboratory of Photonics, Physics Unit, Tampere University, P.O. Box 692, 33014 Tampere, Finland*
[5]*Elettra-Sincrotrone Trieste, 34149 Trieste, Italy*
Corresponding author: antti.kivimaki@maxiv.lu.se

Abstract

We have studied the dissociation of the trifluoromethane molecule, CHF_3, into negative ionic fragments at the C 1s and F 1s edges. The measurements were performed by detecting coincidences between negative and positive ions. We observed five different negative ions: F^-, H^-, C^-, CF^-, and F_2^-. Their production was confirmed by the analysis of triple coincidence events (negative-ion/positive-ion/positive-ion or NIPIPI coincidences), whose signals were cleaner than those of negative-ion/positive-ion coincidences. The intensities of the most intense NIPIPI coincidence channels were recorded as a function of photon energy across the C 1s and F 1s excitations and ionization thresholds. We also observed dissociation channels where one negative ion and three positive ions were formed. The results show that negative-ion/positive-ion coincidence spectroscopy is a very sensitive method to observe anions, which at inner-shell edges are up to three orders of magnitude less probable dissociation products than cations.

1. Introduction

Processes involving the excitation and ionization of K-shell electrons of trifluoromethane (CHF_3), also known as fluoroform, have been studied surprisingly seldom. The C 1s and F 1s ionization energies have been determined to be 299.14(3) eV (an adiabatic value)[1] and 694.1 eV,[2] respectively. In the series of methane and fluorinated methanes, CH_nF_{4-n} (n=0-4), the C 1s and F 1s absorption features nicely shift toward higher energies when the number of fluorine atoms is increased.[3,4] The carbon 1s photoabsorption spectrum of CHF_3 is characterized by two overlapping broad features, which represent transitions to the empty valence orbitals σ^*e and σ^*a_1, and by several considerably narrower peaks, which arise from transitions to atomic-like Rydberg orbitals. The F 1s absorption spectrum of CHF_3 only shows one distinct and wide feature, which has been assigned to the F 1s$\rightarrow \sigma^*$ transition.[4] Ueda *et al*.[4] also reported resonant and normal Auger electron spectra of CHF_3 and CH_3F at selected core excitations and in the core ionization continuum. These spectra arise when the core-hole is filled by a valence electron and another valence electron is emitted (and its kinetic energy is measured), leading to singly charged final states in the case of resonant Auger decay and doubly charged final states in the case of normal Auger decay. Since the ground state of the

CHF_3^+ ion is not stable,[5] the parent molecular ion produced in any kind of Auger processes dissociates immediately. Ion-mass spectroscopy studies of CHF_3 using low-energy electron impact ionization have revealed the cations CF_n^+ (n=1-3), CHF_n^+ (n=1,2), F^+, C^+, and H^+ (e.g., [6]). To our knowledge, fragmentation of CHF_3 following core excitation and core ionization has not been reported in the literature. However, such a study has been carried out for the resembling CF_4 molecule,[7] discovering all possible singly charged cations (except for the parent ion, which is unstable), several dications (C^{2+}, F^{2+}, CF^{2+}, CF_2^{2+} and CF_3^{2+}), and even negative ions (C^-, F^- and CF^-). The appearance of dications can be explained by Auger processes, where two or even three electrons are emitted simultaneously, or by Auger cascades, where the final states of the first-step Auger decay in the parent molecular ion are so highly excited that they decay further by second-step Auger decay, or by autoionization in excited singly charged fragments.

We have recently studied fragmentation channels involving negative ions at the core edges of water, formic acid and methanol.[8-10] Our experimental setup consists of two time-of-flight (TOF) spectrometers;[11] one of the TOF spectrometers is used to detect positive ions, the other is for negative ions. Electrons, which often interfere with negative ion detection, are deflected by a weak magnetic field that is created by permanent magnets, placed outside the vacuum chamber. The set-up has proven to be very sensitive when operated in a measurement mode where negative and positive ions are detected in coincidence. For instance, in the methanol molecule we observed C^- and CH^- ions[10] that had not been found in earlier partial ion yield measurements using a 180º magnetic mass spectrometer.[12] Another proof of sensitivity is that we have been able to observe coincidences between one negative ion and up to three positive ions in methanol and formic acid.[9,10] The relative intensities of the cations and anions can be appreciated from the study of Stolte *et al.*[13]: at the O 1s edge of water, the intensities of O^+ and H^+ were found to be 2-3 orders of magnitude higher than those of the corresponding anions O^- and H^-.

The coincidence detection of negative and positive ions not only helps us to identify negative ions that are released by a given sample molecule, but it also gives information on dissociation channels that produce these anions. In formic acid and methanol, we have found that the $CHOOH^+$ and CH_3OH^+ parent ions, resulting from resonant Auger decay, can dissociate in at least 21 and 29 different ways involving anions, respectively.[9,10] The balance of charges dictates that if an anion is released in dissociation, the other fragments must carry a total charge of +2e after resonant Auger decay and +3e after normal Auger decay. Our studies so far have shown that singly charged cations are greatly favoured in molecular fragmentation processes involving anions. Negative-ion/dication coincidences are negligible in formic acid and methanol;[9,10] however, H^-/O^{2+} is a fairly important channel in water,[8] perhaps due to the smaller number of atoms present in the molecule.

In the present paper, we extend our studies of negative-ion formation in core-excited molecules to CHF_3, a molecule that contains electronegative fluorine atoms. Before performing the experiments, we expected to observe at least four anions (H^-, C^-, F^- and CF^-) and about twenty different NIPIPICO channels. The actual experiments revealed one more anion, F_2^-. In addition to negative-ion/positive-ion coincidence data, we report in this paper the partial positive ions yields of CHF_3 at the C 1s edge.

2. Experimental

The experiments were performed at the Gas Phase Photoemission beamline[14] of the Elettra synchrotron radiation facility. The beamline receives undulator radiation in the photon energy range 13.5-900 eV. Radiation is monochromatized using a spherical grating monochromator, equipped with five interchangeable gratings to guarantee a high (~10^4) resolving power in the whole operation range. The present experiments were carried out with the photon energy resolution of ~40 meV at the C 1s edge and of ~120 meV at the F 1s edge. The photon energy was calibrated at the C 1s edge using the energies of the C 1s excitations of the CO_2 molecule [15] and at the F 1s edge, approximately, using the energy scale given in Ref. 4.

CHF_3 gas was inserted into the experimental chamber through a hypodermic needle whose tip was carefully placed slightly below the monochromatized photon beam. The pressure in the experimental chamber was about $3 \cdot 10^{-7}$ mbar during the experiments, but the local pressure in the interaction region was expected to be 10-50 times higher. Positive and negative ions resulting from the interaction of photons with sample molecules were extracted by a constant electric field towards the two TOF spectrometers. The limiting factor for the collection efficiency was the cutoff kinetic energy of 5.5 eV for positive ions;[9] faster cations with the momentum oriented perpendicularly to the TOF axis could escape the detection. The TOF spectrometers faced each other and both were placed at the angle of 54.7° with respect to the electric vector of the linearly polarized synchrotron radiation in order to avoid angular effects in the measured ion intensities.[16] The contribution of electrons in the negative particle signal was minimized by placing small permanent magnets in suitable positions outside the vacuum chamber. The magnets were removed when positive ions were measured in coincidence with electrons.

In the NIPICO experiments, we do not measure the flight times of negative ions directly but rather establish the presence of anions from arrival time differences (ATDs) between negative and positive ions. In practice, an external pulse generator gives time stamps at a chosen frequency (typically 10 Hz) and the arrival times of negative and positive ions occurring within a pre-selected time (we used 80 ms) of these time stamps are written in a data file. The arrival times are analysed afterwards using a specifically written routine in the data analysis program Igor. This arrangement also allows for the possibility that a negative ion can arrive either before or after the positive ions, depending on their masses. The analysis can thus yield negative-ion/positive-ion coincidences (NIPICO), negative-ion/positive-ion/positive-ion coincidences (NIPIPICO), and so on. For the photoelectron/positive-ion coincidence (PEPICO) measurements, which we employed to measure the partial positive ion yields, the wiring was changed so that electron signals were directly used as start signals and positive ion signals as stop signals (i.e., the pulse generator was not used).

3. Results and discussion

3.1. Positive ion yields at the C K edge

Even though the main focus point of our study was on negative-ion formation, we begin by showing the total and partial ion yields of positive ions (Figure 1) recorded at the C 1s edge because negative ions in our experiments were measured in coincidence with positive ions. For the assignment of negative-ion/positive-ion coincidence channels, it is important to know

which positive ions are created upon core excitation. Note however that the relative intensity ratios of the positive ions detected in coincidence with negative ions may differ from those determined from the TOF spectra containing all positive ions.

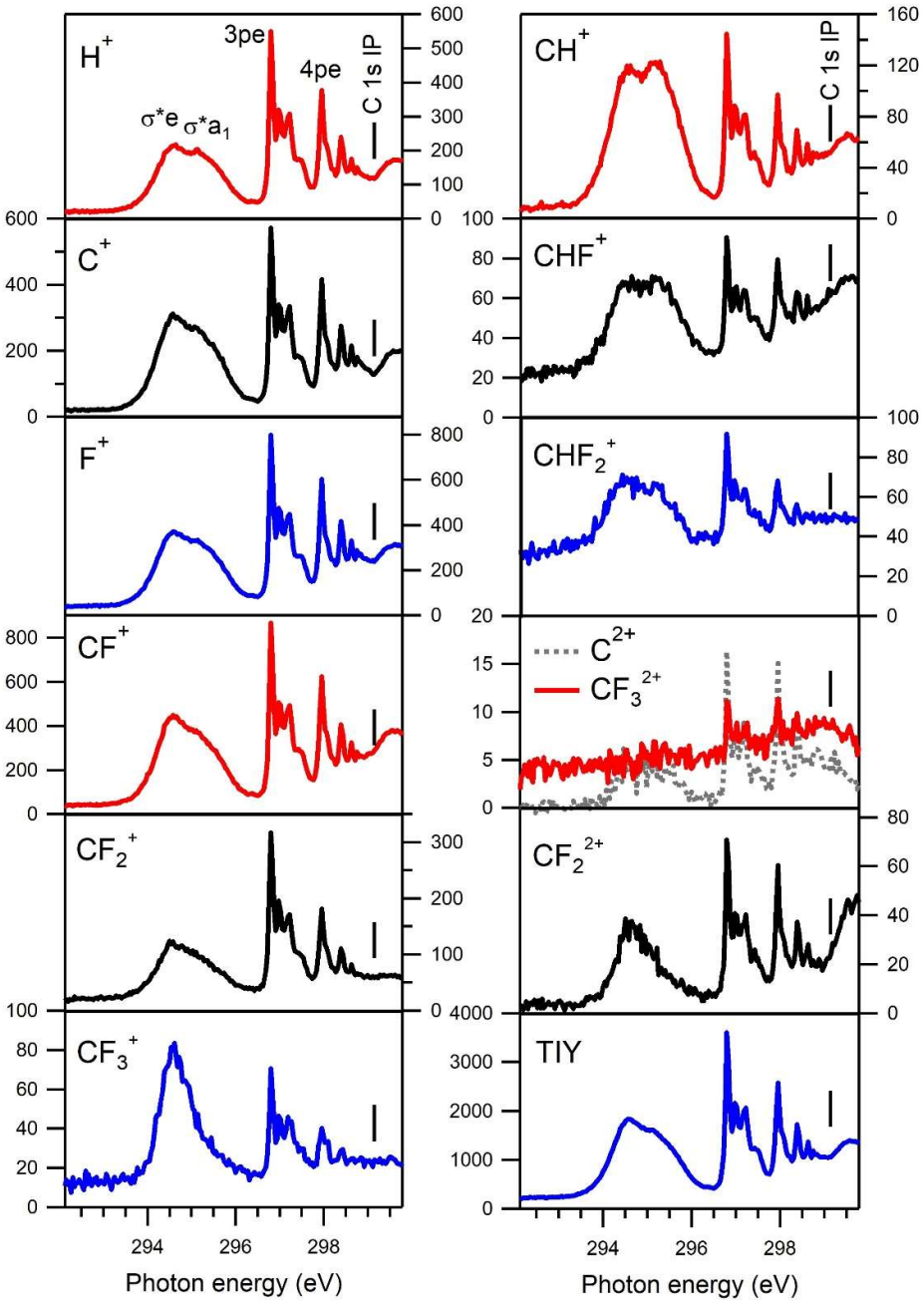

Figure 1. The partial ion yields of positive ions at the C 1s edge. They have been normalized to the photodiode current measured simultaneously. TIY shows the sum of the observed partial ion yields. The main resonances are labelled according to Ref. 4 in the top left panel.

The most probable positively charged fragments after C 1s excitations are F^+ and CF^+, followed by H^+ and C^+. The yields of these four fragments do not show large differences as a

function of photon energy. However, a more careful inspection reveals that the production of H^+ appears slightly suppressed at the σ* excitations (294-296 eV) relative to the Rydberg excitations (296.8-299 eV), when their relative intensities are compared to those in the total ion yield (bottom right in Figure 1). Fast protons can escape detection, so the reduced intensity of H^+ at the σ* excitations could be explained, at least in principle, if H^+ ions received higher kinetic energies in dissociation processes at the σ* excitations than at the Rydberg excitations. Another and more likely possibility is that dissociation following C 1s → σ* excitations simply produces less H^+ ions because we do see variations in relative intensities between the resonances in the case of other fragments (see below), for which ions are not expected to escape detection because of their lower kinetic energies.

When compared to the relative intensities in TIY, the production of CH^+ appears enhanced at the C 1s → σ* resonances and particularly so at C 1s → σ*a_1 resonance. A similar behaviour is visible in the CHF^+ yield. The production of CF_3^+ is the most favoured at the C 1s → σ*e resonance, while it is very weak at the other valence resonance, C 1s → σ*a_1. Thus there are clear differences in fragmentation pathways between the two C 1s → σ* resonances. CF_2^{2+} is the most intense among the dications. Its yield increases above the C 1s IP when normal Auger becomes the main decay channel of core-hole states. The yield of CF_3^{2+} only reveals the Rydberg excitations. In summary, there are many photon energy dependent variations in the partial ion yields of positive ions. Studies of photoelectron/positive-ion/positive-ion coincidences could explain some of these observations. They are, however, beyond the scope of the present paper.

The partial ion yields of positive ions were also measured at the F 1s edge. They are not reported here because they appear to display a structure that is due to an instrumental artefact. However, the same positive ions were observed at the F 1s edge as at the C 1s edge except that the dication F^{2+} appeared as a new fragment at the F 1s edge.

3.2. Identification of negative ions and NIPIPICO channels

Figure 2 shows the arrival time difference spectra constructed by combining the data from several measurements across the C 1s → σ*e and σ*a_1 resonances (solid red curve) and at the F 1s → σ* resonance (black dotted curve). The intensity scale refers to the former curve and it was obtained by binning the arrival time differences within 10 ns wide intervals. The dotted curve has been scaled to the same height at the F^-/H^+ peak (leftmost in the spectrum). These measurements were performed using the same potentials in the TOF spectrometer as in the previous study on methanol.[10] The flight times of the positive and negative ions therefore followed the equations derived in,[10] allowing us to assign readily most peaks in Figure 2 and to calculate the expected positions of any NI/PI coincidence peaks. We have also indicated electron/positive-ion coincidence peaks, which arise due to incomplete removal of electrons by the magnetic field. The positions of some peaks do not match any coincidences; they are labelled with question marks in Figure 2. It appears that some peak-like intensity originated from instrumental artefacts. For instance, no reasonable assignment can be proposed for the peak at -2430 ns (on the right side of the F^-/H^+ peak). On the other hand, this peak completely disappeared after undoing and redoing the electrical connections for the NIPICO measurements at the F 1s edge, suggesting that it was due to problems in connections.

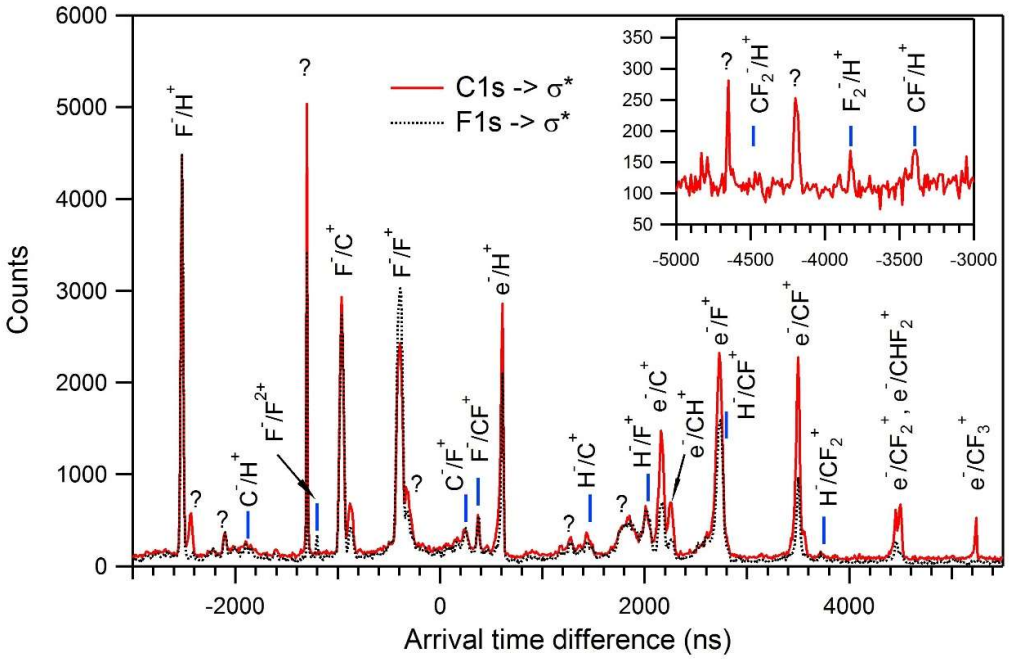

Figure 2. The arrival time difference spectra of CHF_3 constructed from the measurements performed across the C 1s → σ*e and σ*a_1 resonances (solid curve) and across the F 1s → σ* resonance (dotted curve). Blue vertical bars show the expected positions of the indicated NI/PI coincidences. The total measuring time was 6 h for the solid curve and 4 h for the dotted curve.

NIPICO peaks that involve the F^- ion are by far most intense, especially when atomic cations H^+, C^+ and F^+ are detected in coincidence with F^-. The relative intensities of these peaks change noticeably when the core excitation takes place in an F atom. In particular, the F^-/F^+ gains intensity upon going from the C 1s edge to the F 1s edge. At the F 1s edge, the F^-/F^{2+} also becomes visible. NIPICO peaks involving the C^- and H^- ions are about one order of magnitude weaker than those involving the F^- ion.

NI/PI peaks have most negative ATDs when a heavy negative ion is observed in coincidence with H^+. The inset of Figure 2 shows that the expected ATDs of the CF^-/H^+ and F_2^-/H^+ coincidences match very well with the positions of two narrow peaks in the experimental spectrum. This may not yet be a conclusive evidence for the detection of CF^- and F_2^-, as the same temporal region also shows some unknown peaks of larger intensity. However, the observation of both CF^- and F_2^- is confirmed by the NIPIPICO data of Figure 3, where these anions appear in coincidence with two positive ions. It is interesting to note the clear observation of $F_2^-/H^+/C^+$, while the coincidence intensity in the circle corresponding to $F_2^-/H^+/F^+$ is not higher than in the other parts of the diagonal direction along which $NI/H^+/F^+$ coincidences are aligned. CF^- and F_2^- anions have previously been observed in the valence region of the CF_3Cl, CF_3Br and CF_3I molecules.[17] CF^- was also observed at the core edges of CF_4, but F_2^- was not.[7]

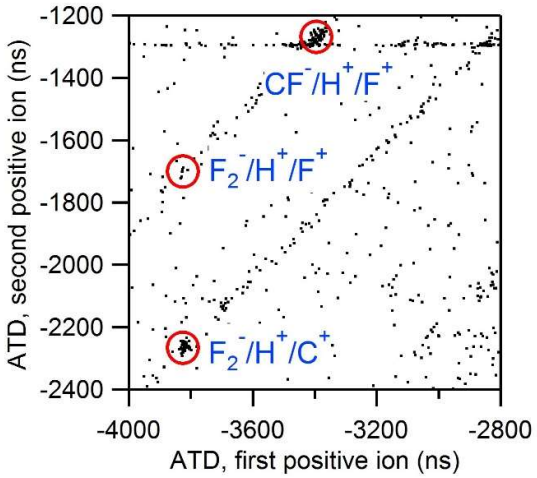

Figure 3. An extract of the NIPIPI coincidence map formed from the data taken across the the C 1s → σ*e and σ*a_1 resonances. It shows the part where coincidences with NI=F_2^- and CF^- are expected. The circles show the expected positions of the indicated NIPIPI coincidences with radius of 50 ns. The measuring time was 6 h.

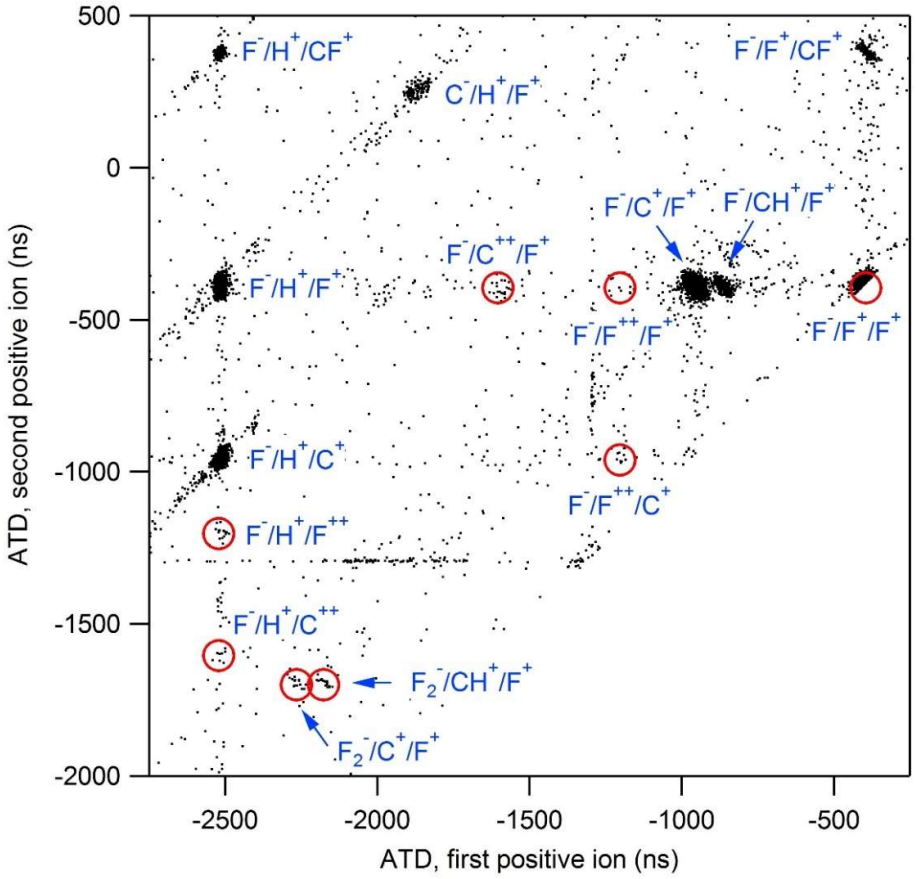

Figure 4. NIPIPICO map formed from the measurements done across the F 1s → σ* resonance. The circles show the expected positions of the indicated NIPIPI coincidences with radius of 50 ns.

A wide-view NIPIPICO map is shown in Figure 4. In order to make also the weakest dissociation channels visible we have added in the analysis all the data measured at different photon energies across the F 1s → σ* resonance. This results in the saturation in areas where most intense NIPIPICO channels produce events; individual dots are no longer distinguishable and relative intensities of different channels cannot be appreciated. We will deal with the relative intensities of some NIPIPICO channels in the next subsection. In Figure 4, coincidence islands arrange themselves in three different directions. In the vertical direction, the negative ion and the first positive ion remain the same, while the coincidence spots move up when the m/q ratio of the second positive ion increases. This is most easily seen by looking at the x-axis value near -2500 ns, which corresponds to the NI/PI_1 pair of F^-/H^+. In the horizontal direction, the negative ion and the second positive ion remain the same, while the spots move to right when the m/q ratio of the first positive ion increases. Finally, the coincidence spots align diagonally, when the two positive ions remain the same and the mass of the negative ion changes (see, for example, $F^-/H^+/F^+$ and $C^-/H^+/F^+$ in the upper left corner of Figure 4).

We have indicated with circles the expected positions of some weaker NIPIPI coincidence channels, in particular of those where C^{2+} and F^{2+} are involved. It is debatable as to which NIPIPICO channels with dicationic participation are really observed in Figure 4, but $F^-/C^{2+}/F^+$ and $F^-/H^+/F^{2+}$ are the strongest candidates. Among the encircled coincidence patterns we also find two more channels with the F_2^- ion: $F_2^-/C^+/F^+$ and $F_2^-/CH^+/F^+$. The latter channel is the only one within Figure 4 that includes all the atoms of the parent molecule. Outside the shown area, another "complete" channel, $F^-/H^+/CF_2^+$ is not observed at the F 1s edge, but could be weakly present at the C 1s → σ*e and σ*a_1 resonances. Finally, we have also encircled the expected position of the $F^-/F^+/F^+$ channel. This illustrates the case where the MCP detector cannot register two F^+ ions if they arrive too close in time within each other. The intensities of all dissociation channels with two F^+ ions are therefore underestimated in our experiments.

All NIPIPICO channels with NI=H^- are outside the shown area of Figure 4. As can be expected from Figure 2, they are on average much weaker than the NIPIPICO channels with NI=F^-. We limit ourselves here to give the list of the observed H^- channels: $H^-/C^+/F^+$, $H^-/F^+/F^+$, $H^-/F^+/CF^+$ and $H^-/F^+/CF_2^+$. The latter contains all the atoms of the parent molecule. A NIPIPICO channel with the C^- ion is visible in the upper part of Figure 4: $C^-/H^+/F^+$. Additionally we observed another C^- channel: $C^-/F^+/F^+$. Dications were not observed together with H^- or C^-.

3.3. NIPIPICO yields

Figure 5 shows the yields of the three most intense NIPIPICO channels involving F^- as well as of the most intense non-F^- NIPIPICO channel, $C^-/H^+/F^+$, across the C 1s excitations. They are compared to the total positive ion yield, which has been scaled to have approximately the same intensity as the $F^-/H^+/C^+$ and $F^-/C^+/F^+$ channels at the C 1s → σ*e and σ*a_1 resonances. All the NIPIPICO channels shown become more intense at Rydberg excitations (like 3pe and 4pe) than at the valence resonances σ*e and σ*a_1. The intensity increase at Rydberg excitations is larger for the $F^-/C^+/F^+$ channel than for the $F^-/H^+/C^+$ channel. We attribute the observation to the increased negative ion formation at the C 1s → Rydberg excitations, even

though it could also be explained, at least in principle, if positive ions had considerably smaller kinetic energies at the Rydberg excitations than at the valence resonances.

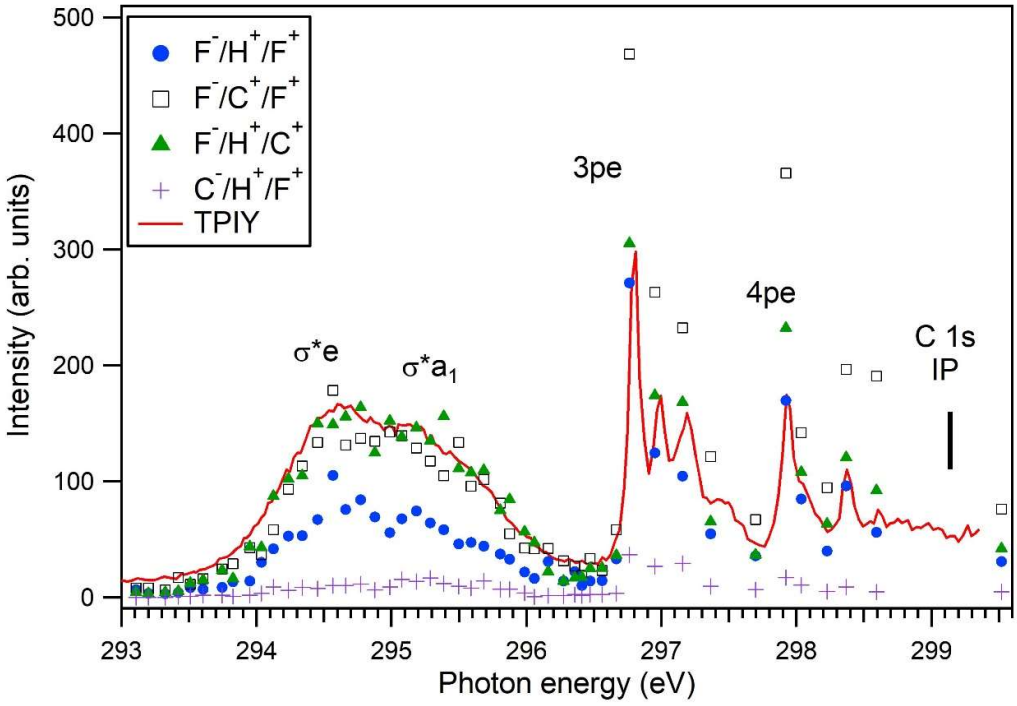

Figure 5. Selected NIPIPI coincidence yields at the C 1s edge in comparison with the total positive ion yield (TPIY). The assignments of the resonances are from Ueda *et al.* [4]. Negative ion formation is more probable at the Rydberg excitations than at the σ* resonances.

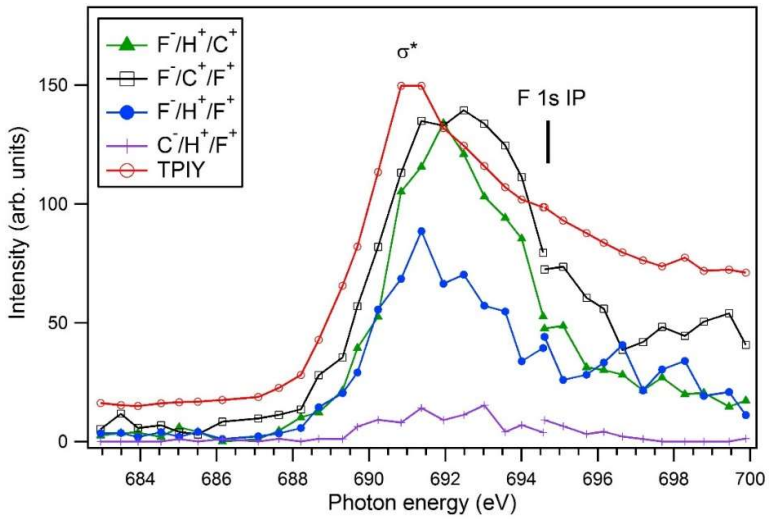

Figure 6. Selected NIPIPI coincidence yields at the F 1s edge in comparison with the total positive ion yield (TPIY) measured simultaneously. The assignment and approximate energy calibration are from Ref. [4].

Figure 6 shows the same NIPIPICO yields at the F 1s edge together with the total positive ion yield (TPIY) measured simultaneously. The latter only displays one feature, which has been assigned to the F 1s → σ* resonance.[4] The NIPIPICO yields seem to peak at higher energies than the TPIY. This could indicate the contribution of unresolved Rydberg excitations between the σ* maximum and the F 1s ionization potential, if we assume that Rydberg character in the core-excited state increases negative ion formation as it does at the C 1s edge. The intensity order of the different NIPIPICO channels is the same at the F 1s edge as at the C 1s edge.

3.4. NIPIPIPI coincidences

In order to check whether we can observe four-ion coincidences (one negative ion, three positive ions) we performed the analysis on the data set comprising measurements done at different photon energies across the C 1s → σ*e and σ*a_1 resonances and at the F 1s → σ* resonance. Figures 7 and 8 show the results of the analysis that only used events where 4 particles had been observed within a short time interval. The main panel shows the arrival time difference (ATD) spectrum of the first positive ion with respect to the negative ion. We can observe that the F^-/H^+ ion pair is the most likely combination and we have performed the further analysis only for that peak. (Referring to Figure 2, the peaks at ~-900 ns and ~-400 ns correspond to F^-/C^+ and F^-/F^+ ion pairs, respectively, in Figures 7 and 8.) The insets thus show the PI_2/PI_3 coincidences only in the case where NI/PI_1 have been restricted to be F^-/H^+. The $F^-/H^+/C^+/F^+$ channel is observed to be a strong NIPIPIPICO channel. Its relative intensity with respect to the $F^-/H^+/F^+/F^+$ channel could not be determined because in the latter case many events may have escaped registration due to the dead time of the detector. We also observe few events in the $F^-/H^+/F^+/CF^+$ channel, where all constituent atoms of the parent molecule are included.

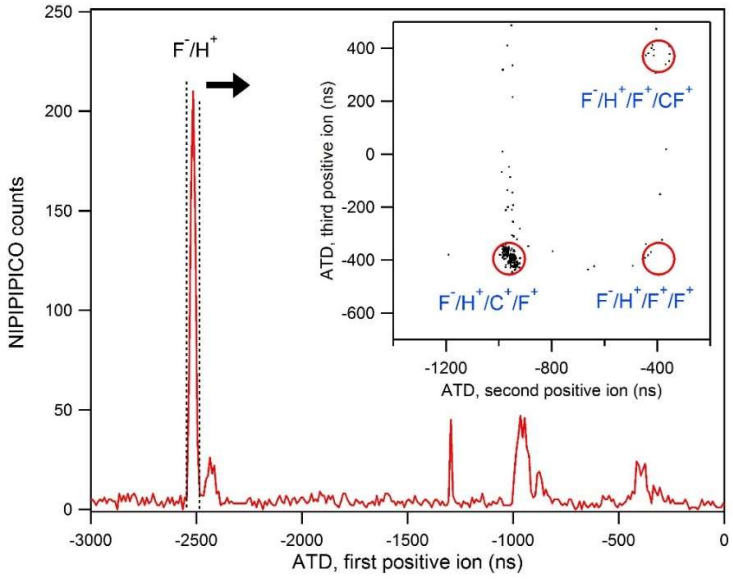

Figure 7. NIPIPIPICO spectrum at the C 1s → σ*e and σ*a_1 resonances (6 h measuring time). The main panel shows the arrival time difference (ATD) spectrum of the first positive ion extracted from the events where one negative ion and three positive ions were detected in

coincidence. The inset shows the ATD of the third positive ion (PI_3) vs that of the second positive ion (PI_2) among those $NIPI_1PI_2PI_3$ events where NI/PI_1 has been preselected to be F^-/H^+ (the peak between the dotted vertical lines in the main panel). The circles show the expected positions of PI_2/PI_3 coincidences within the radius of 60 ns.

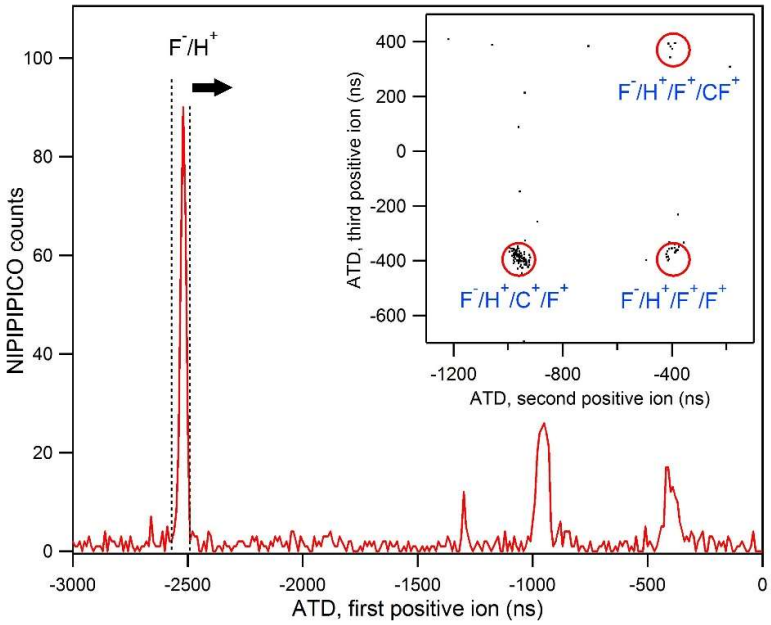

Figure 8. NIPIPIPICO spectrum measured across the F 1s → σ* resonance (4 h measuring time). See Figure 7 caption for details of the analysis.

Figure 8 shows more $F^-/H^+/F^+/F^+$ coincidences than Figure 7, which could be due to higher kinetic energies (and bigger flight time differences) of the F^+ ions at the F 1s edge. Similar analysis of the NI/PI_1 peak around -1000 ns (F^-/C^+) in the main panel of Fig. 8 only shows $F^-/C^+/F^+/F^+$ coincidences, a large fraction of which could have been lost due to the dead time of the MCP detector.

4. Conclusions

We have studied the dissociation of the CHF_3 molecule into positively and negatively charged fragments following K-shell photoexcitation and photoionization. The used negative-ion/positive-ion coincidence (NIPICO) technique can distinguish very weak dissociation channels. It is therefore well suited to determine which anionic species are present among the dissociation products. We found five anionic fragments: F^-, H^-, C^-, CF^- and F_2^-, among which F^- is by far the most probable. Coincidence detection of a negative ion with two positive ions (i.e., NIPIPICO or negative-ion/positive-ion/positive-ion coincidences) confirmed the appearance of the CF^- and F_2^- ions. In total, about 20 different NIPIPICO channels were observed. The intensities of four NIPIPICO channels were followed as a function of photon energy across the C 1s and F 1s resonances and ionization potentials. Negative ion production was found to be slightly more probable at core-to-Rydberg resonances than at core-to-valence resonances. Summing up all recorded data, irrespective of photon energy at a given core edge,

gave evidence of dissociation channels involving one negative ion and three positive ions (NIPIPIPICO channels). As a by-product of this study, we also reported the yields of the positive ions across the C 1s edge of CHF_3.

References

[1] Myrseth V, Bozek JD, Kukk E, Sæthre LJ, Thomas TD. Adiabatic and vertical carbon 1s ionization energies in representative small molecules. *J. Electron Spectrosc. Relat. Phenom*. **2002**, *122*, 57.

[2] Thomas TD. X-ray photoelectron spectroscopy of simple hydrocarbons. *J. Chem. Phys*. **1970**, *52*, 1373.

[3] Brown FC, Bachrach RZ, Bianconi A. Fine structure above the carbon K-edge in methane and in the fluoromethanes. *Chem. Phys. Lett*. **1978**, *54*, 425.

[4] Ueda K, Shimizu Y, Chiba H, Okunishi M, Ohmori K, Sato Y, Shigemasa E, Kosugi N. C 1s and F 1s photoabsorption and subsequent electronic decay of CH_4, CH_3F, CH_2F_2, CHF_3, and CF_4. *J. Electron Spectrosc. Relat. Phenom.* **1996**, *79*, 441.

[5] McKoy BV, as cited in Jiao CQ, Nagpal R, Haaland PD. Ion chemistry in trifluoromethane, CHF_3. *Chem. Phys. Lett.* **1997**, *269*,117.

[6] Iga I, Sanches IP, Srivastava SK, Mangan M. Electron impact ionization of CHF_3. *Int. J. Mass Spectrom.* **2001**, *208*, 159.

[7] Guillemin R, Stolte WC, Piancastelli MN, Lindle DW. Jahn-Teller coupling and fragmentation after core-shell excitation in CF_4 investigated by partial-ion-yield spectroscopy. *Phys. Rev. A.* **2010**, *82*, 043427.

[8] Stråhlman C, Kivimäki A, Richter R, Sankari R. Negative-ion/positive-ion coincidence yields of core-excited water. *J. Phys. Chem A.* **2016**, *120*, 6389.

[9] Stråhlman C, Kivimäki A, Richter R, Sankari R. Negative- and positive-ion fragmentation of core-excited formic-acid molecules studied with three- and four-ion coincidence spectroscopy. *Phys. Rev. A.* **2017**, *96*, 023409.

[10] Kivimäki A, Stråhlman C, Richter R, Sankari R. Fragmentation of methanol molecules after core excitation and core ionization studied by negative-ion/positive-ion coincidence experiments. *J. Phys. Chem A.* **2018**, *122*, 224.

[11] Stråhlman C, Sankari R, Kivimäki A, Richter R, Coreno M, Nyholm R. *Rev. Sci. Instrum.* **2016**, *87*, 013109.

[12] Stolte WC, Öhrwall G, Sant'Anna MM, Dominguez Lopez I, Dang LTN, Piancastelli MN, Lindle DW. 100% site-selective fragmentation in core–hole-photoexcited methanol by anion-yield spectroscopy. *J. Phys. B.* **2002**, *35*, L253.

[13] Stolte WC, Sant'Anna MM, Öhrwall G, Dominguez-Lopez I, Piancastelli MN, Lindle DW. Photofragmentation dynamics of core-excited water by anion-yield spectroscopy. *Phys. Rev. A.* **2003**, *68*, 022701.

[14] Prince KC, Blyth RR, Delaunay R, et al. The Gas-Phase Photoemission beamline at Elettra. *J. Synchrotron Radiat.* **1998**, *5*, 565.

[15] Prince KC, Avaldi L, Coreno M, Camilloni R, de Simone M. Vibrational structure of core to Rydberg excitations of carbon dioxide and dinitrogen oxide. *J. Phys. B*. **1999**, *32*, 2551.

[16] Morin P, Nenner I, Guyion PM, Dutuit O, Ito K. Time of flight photoelectron spectroscopy using synchrotron radiation study of resonances in O_2. *J. Chim. Phys*. **1980**, *77*, 605.
[17] Simpson MJ, Tuckett RP. Vacuum-UV negative photoion spectroscopy of gas-phase polyatomic molecules. *Int. Rev. Phys. Chem*. **2011**, *30*, 197.